Journal of Theoretical and Applied Physics
a SpringerOpen Journal

RESEARCH Open Access

Recombination phenomenon in polyethylene under space charge dynamics and its effects on the external current evolution

Imed Boukhris*, Amal Gargouri, Ezzeddine Belgaroui and Ali Kallel

Abstract

This paper presents bipolar transport model results concerning the recombination phenomenon in a low-density polyethylene under direct current (dc) applied voltages. Results obtained indicate the existence of a threshold value of voltage between two different space charge dynamics. Indeed, we show that under low dc applied voltage, the total recombination rate density is dominated by the recombination between trapped electrons and trapped holes, while under high dc voltage, the recombination is governed by mobile electron-trapped hole and trapped electron-mobile hole recombinations. This is due to the fact that under low dc voltage, trapped charges dominate, while under high voltage, mobile charge density is much higher. In addition, we show the significant effect of the recombination phenomenon on the external current evolution at transient and steady states.

Keywords: Bipolar transport model, Polyethylene, Space charge, Recombination phenomenon, External current, Dc voltage

Archive of SID

Introduction

Low-density polyethylene (LDPE) is widely used as an electrical insulating material in underground distribution and transmission cables because of its excellent dielectric proprieties [1,2]. Unfortunately, several technical tests often showed the existence of the electrical breakdown phenomenon which occurs during the application of a direct current (dc) voltage [3,4]. Nowadays, it is well known that these problems are often allotted to the accumulation and the evolution of the space charges in the insulating materials [5-7]. With an aim of studying the accumulation and the dynamics of these charges, several experimental characterizations were developed during these last year's [8-10].

Since the beginning of the 1990s, physical modeling and numerical methods of resolution were integrated for a better comprehension of the behavior of the space charge generated in the case of bipolar transport under dc voltage [11-16]. The numerical methods give access to certain specific physical sizes such as the densities of each type of carrier in a material. These densities constitute the components of the net charge density and are then more favorable to explain certain physical phenomena such as the recombination rate density and the external current [17].

In this paper, we present new numerical results carried out by our bipolar transport model [16] for both the transient and the steady state regimes. First, we show principally the space charge dynamic under low and high dc applied voltage. Next, we show the evolutions of the total recombination rate density as well as the different types of recombination. Finally, we investigate especially the effects of the recombination phenomenon on the transient and steady states of the external current.

Theoretical approach

Basic equations and boundary conditions

The physical model regroups Poisson's, the continuity and the transport equations. In Poisson's equation, the initial and the boundary conditions are given as follows:

$$\frac{\partial^2 V(x,t)}{\partial x^2} + \frac{\rho(x,t)}{\varepsilon} = 0 \qquad 0 < x < D \tag{1}$$

$$\text{grad}\ (V(x,t)) = -E(x,t), \tag{2}$$

* Correspondence: imed_boukhris@yahoo.fr
Laboratoire des matériaux composites céramiques et polymères (LaMaCoP), Faculté des sciences de Sfax, BP 805, Sfax 3000, Tunisia

Springer

© 2013 Boukhris et al.; licensee Springer. This is an Open Access article distributed under the terms of the Creative Commons Attribution License (http://creativecommons.org/licenses/by/2.0), which permits unrestricted use, distribution, and reproduction in any medium, provided the original work is properly cited.

www.SID.ir

where $V(x,t)$, $E(x,t)$, and $\rho(x,t)$ are the local potential, the electric field, and the net charge density, respectively.

The initial condition for the free additive polyethylene film is as follows:

$$\rho(x,0) = 0. \tag{3}$$

The boundary conditions are written as follows:

$$\Delta V = V_C - V_A \tag{4}$$

$$V(0, t>0) = V_C \tag{5}$$

$$V(D, t>0) = V_A \tag{6}$$

$$\int_0^D E\, dx = \Delta V, \tag{7}$$

where V_C and V_A are the potentials at the cathode and anode, respectively, and D is the dielectric thickness.

The continuity equation, with trapping and recombination term sources, as well as the transport equation is given as follows:

$$\frac{\partial \rho_{(e,h)\mu}(x,t)}{\partial t} + \frac{\partial j_{(e,h)}(x,t)}{\partial x} = S_{t(e,h)}(x,t) + S_{r(e,h)}(x,t) \tag{8}$$

$$j_{(e,h)}(x,t) = \mu_{e,h}\ \rho_{(e,h)\mu}(x,t) E(x,t) \tag{9}$$

where μ_{eh} is the mobility of carrier, and $\rho_{e\mu}(x,t)$ and $\rho_{h\mu}(x,t)$ are the densities of the mobile electrons and holes, respectively. $j_{(e,h)}(x,t)$ is the flux of the mobile electrons or holes. $S_{t(e,h)}(x,t)$ and $S_{r(e,h)}(x,t)$ are the trapping and the recombination source terms for the electrons or the holes [12].

The net charge density $\rho(x,t)$ is locally composed of the mobile and the trapped carriers. This density is defined as follows:

$$\rho(x,t) = \rho_{h\mu}(x,t) + \rho_{ht}(x,t) - \rho_{e\mu}(x,t) - \rho_{et}(x,t), \tag{10}$$

where $\rho_{et}(x,t)$ and $\rho_{ht}(x,t)$ are the densities for the trapped electrons and holes, respectively.

The boundary conditions for the injected charges are represented by the Schottky law:

$$j_e(0,t) = AT^2 \exp\left(-\frac{w_{ei}}{kT}\right)\ \exp\left(\frac{e}{kT}\sqrt{\frac{e|E(0,t)|}{4\pi\varepsilon}}\right) \tag{11}$$

$$j_h(D,t) = AT^2 \exp\left(-\frac{w_{hi}}{kT}\right)\ \exp\left(\frac{e}{kT}\sqrt{\frac{e|E(D,t)|}{4\pi\varepsilon}}\right), \tag{12}$$

where $j_e(0,t)$ and $j_h(0,t)$ are the fluxes of electrons and holes at the cathode and anode, respectively, T is the temperature of the sample, and A is the Richardson constant which is equal to 1.2×10^6 A m^{-1} K^{-2}. w_{ei} and w_{hi} are the injection barriers for the electrons and the holes, respectively.

Equations for the recombination rate and the current densities

The recombination rate equations

The total recombination rate equation is as follows:

$$S_r(x,t) = S_{r(e\mu,ht)}(x,t) + S_{r(et,h\mu)}(x,t) + S_{r(et,ht)}(x,t). \tag{13}$$

The recombination rate equation for mobile electron and trapped hole is written as follows:

$$S_{r(e\mu,ht)}(x,t) = -s_1\, \rho_{e\mu}(x,t)\, \rho_{ht}(x,t), \tag{14}$$

where s_1 is the recombination coefficient for mobile electron and trapped hole.

The recombination rate equation for trapped electron and mobile hole is represented by

$$S_{r(et,h\mu)}(x,t) = -s_2\, \rho_{et}(x,t)\, \rho_{h\mu}(x,t), \tag{15}$$

where s_2 is the recombination coefficient for trapped electron and mobile hole.

The recombination rate equation for trapped electron and trapped hole is as follows:

$$S_{r(et,ht)}(x,t) = -s_0\, \rho_{et}(x,t)\, \rho_{ht}(x,t), \tag{16}$$

where s_0 is the recombination term source for trapped electron and trapped hole.

Equations of the variation of charge densities

The source terms of recombination and trapping learn about the variation (disappearance or appearance) in densities of each type of mobile and trapped carriers. These variations are represented by the following equations:

- Variation of mobile electron density:

$$\frac{\partial\ \rho_{e\mu}(x,t)}{\partial\ t} = \underbrace{-s_1\ \rho_{e\mu}(x,t)\ \rho_{ht}(x,t)}_{\text{Disappearance by recombination with trapped holes}} \underbrace{-B_e\ \rho_{e\mu}(x,t)\left(1 - \frac{\rho_{et}(x,t)}{\rho_{Te}(x,t)}\right)}_{\text{Disappearance by trapping}} \tag{17}$$

Archive of SID
www.SID.ir

- Variation of mobile hole density:

$$\frac{\partial\ \rho_{h\mu}(x,t)}{\partial\ t} = \underbrace{-s_2\ \rho_{h\mu}(x,t)\quad \rho_{et}(x,t)}_{\text{Disappearance by recombination with trapped electrons}} \underbrace{-\ B_h\ \rho_{h\mu}(x,t)\left(1-\frac{\rho_{ht}(x,t)}{\rho_{Th}}\right)}_{\text{Disappearance by trapping}} \tag{18}$$

- Variation of trapped electron density:

$$\frac{\partial\rho_{et}(x,t)}{\partial\ t} = \underbrace{-s_0\rho_{et}(x,t)\rho_{ht}(x,t)}_{\text{Disappearance by recombination with trapped holes}} - \underbrace{s_2\rho_{ht}(x,t)\rho_{h\mu}(x,t)}_{\text{Disappearance by recombination with mobile holes}} \underbrace{+\ B_e\rho_{e\mu}(x,t)\left(1-\frac{\rho_{et}(x,t)}{\rho_{Te}}\right)}_{\text{Appearance with trapping}} \tag{19}$$

- Variation of trapped hole density:

$$\frac{\partial\rho_{ht}(x,t)}{\partial\ t} = \underbrace{-s_0\rho_{et}(x,t)\rho_{ht}(x,t)}_{\text{Disappearance by recombination with trapped electrons}} - \underbrace{s_1\rho_{e\mu}(x,t)\rho_{ht}(x,t)}_{\text{Disappearance by recombination with mobile electrons}} \underbrace{+\ B_h\rho_{h\mu}(x,t)\left(1-\frac{\rho_{ht}(x,t)}{\rho_{Th}}\right)}_{\text{Appearance by trapping}} \tag{20}$$

To recapitulate, we present in Figure 1 a schematic of the mechanism of conduction taking into account trapping and recombination phenomena.

Current densities

The instantaneous local conduction current density for the mobile electron and hole is written as follows:

$$j_{e\mu,h\mu}(x,t) = \left(\mu_e\ \rho_{e\mu}(x,t) + \mu_h\ \rho_{h\mu}(x,t)\right)E(x,t). \tag{21}$$

The instantaneous local displacement current density is

$$j_d(x,t) = \varepsilon\frac{\partial E(x,t)}{\partial t}. \tag{22}$$

The external current density, obtained by numerical integration, is

$$J(t) = \int_0^D \left(j_{e\mu,h\mu}(x,t) + j_d(x,t)\right)\quad dx. \tag{23}$$

Because of the stationary boundary Equation 7, the following condition is always satisfied:

$$\int_0^D j_d(x,t)\ dx = 0. \tag{24}$$

The nomenclature of different model coefficients and parameters is given in Table 1, and all the parameter values used in this work are regrouped in Table 2 [11,16].

Results and discussion

Before presenting our model results, we note that our model was already experimentally validated, and it is in good agreement with the experimental results concerning the external current density and the conduction current density. Indeed, our model gives quantitatively and qualitatively regular evolutions of the external current density under different applied electric fields [18] and of the conduction current density at transient and steady states at different temperatures [19].

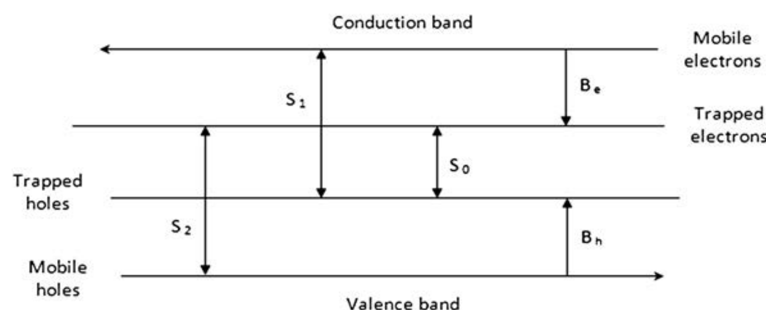

Figure 1 Schematic of the conduction mechanism.

Archive of SID
www.SID.ir

Table 1 Nomenclature

	Nomenclature	Unit
Local potential	V	V
Electric field	E	$V{\cdot}m^{-1}$
Net charge density	ρ	$C{\cdot}m^{-3}$
Dielectric permittivity	ε	$A{\cdot}s{\cdot}V^{-1}{\cdot}m^{-1}$
Potential at the cathode	V_C	V
Potential at the anode	V_A	V
Dielectric thickness	D	m
Mobility of carriers	μ	$m^2{\cdot}V^{-1}{\cdot}s^{-1}$
Mobile electron density	$\rho_{e\mu}$	$C{\cdot}m^{-3}$
Mobile hole density	$\rho_{h\mu}$	$C{\cdot}m^{-3}$
Trapped electron density	ρ_{et}	$C{\cdot}m^{-3}$
Trapped hole density	ρ_{ht}	$C{\cdot}m^{-3}$
Mobile electron or hole charge flux	$j_{(e\ (or)\ h)}$	V·m
Trapping source terms	$S_{t(e\ (or)\ h)}$	$m^3{\cdot}C^{-1}$
Recombination source terms	$S_{r(e\ (or)\ h)}$	$m^3{\cdot}C^{-1}$
Trapping coefficients	$B_{(e\ (or)\ h)}$	s^{-1}
Recombination coefficients	$S_{(et\ (or)\ e\mu,\ h\mu\ (or)\ ht)}$	$m^3{\cdot}C^{-1}$
Density of traps	ρ_{Te} and ρ_{Th}	
Flux of electrons at the cathode	$j_e(0,t)$	V·m
Flux of holes at the anode	$j_h(D,t)$	V·m
Temperature	T	K
Richardson constant	A	$A{\cdot}m^{-2}{\cdot}K^{-2}$
Injection barrier for the electrons	w_{ei}	eV
Injection barrier for the holes	w_{hi}	eV

Table 2 Parameters of the model

Parameters	Fixed values
Coefficients of trapping	
B_e (electrons)	$7 \times 10^{-3}\ s^{-1}$
B_h (holes)	$7\times 10^{-3}\ s^{-1}$
Coefficients of recombination	
S_0 (trapped electron-trapped hole)	$4 \times 10^{-3}\ m^3\ C^{-1}\ s^{-1}$
S_1 (mobile electron-trapped hole)	$4 \times 10^{-3}\ m^3\ C^{-1}\ s^{-1}$
S_2 (trapped electron-mobile hole)	$4 \times 10^{-3}\ m^3\ C^{-1}\ s^{-1}$
S_3 (mobile electron-mobile hole)	Neglected (=0)
Mobilities	
μ_e (electron)	$9 \times 10^{-15}\ m^2\ V^{-1}\ s^{-1}$
μ_h (hole)	$9 \times 10^{-15}\ m^2\ V^{-1}\ s^{-1}$
Trap density	
dpe (electrons)	$100\ C\ m^{-3}$
dpt (holes)	$100\ C\ m^{-3}$
Injection barriers	
w_{ei} (electrons)	1.2 eV
w_{hi} (holes)	1.2 eV
Temperature	25°C
Applied voltage	10 and 50 kV
Time step	0.01 s
Sample thickness	150 μm
Spatial discretization	Variable

Space charge dynamics under low and high dc applied voltage

We showed in our previous modeling works the existence of a threshold value of voltage which separates two different charge dynamics [16,20]. We proved that the charge dynamic is controlled by the type of charge dominating. Indeed, under low applied voltage, this dynamic is governed by trapped charges; however, it is controlled by mobile carriers in the case of high voltage [20].

In the following sections, we investigate the recombination phenomenon by examining the dominant type of recombination under low and high dc applied voltage: trapped electron-trapped hole (S_0), mobile electron-trapped hole (S_1), and trapped electron-mobile hole (S_2).

Recombination evolutions under space charge dynamics

Figure 2 shows the total recombination rate density in a LDPE under a 50-kV dc applied voltage. During the transient state, we remark that the recombination phenomenon appears after 50 s at the center of the sample, and then two peaks appear and progressively move towards the electrodes as seen at 80 s. These peaks are attributed to the mobile charge packets which are considered as dominants in the total recombination rate between electrons and holes [16]. For more explanation of these aspects, we show in Figure 3a,b the densities of mobile electrons and mobile holes under 50 kV, respectively. This figure indicates that packets of mobile electrons and mobile holes reach the center of the sample after 50 s which proves the apparition of the maximum on the profile of the total recombination rate density at 50 s. After that (80 s), packets of mobile electrons and holes move towards the opposite electrode which proves the two peaks observed on the total recombination rate density. At steady state, profiles have concavities that turn to high rates of recombination density (profile 500 s), and the recombination rate is highly confined close to the electrodes: the high production of the injected mobile charges at the anode and the cathode under high dc voltage [20]. These results are in a good agreement with those obtained by the steady model of Baudoin [17].

Figure 4a,b shows the recombination rate density between mobile electron-trapped hole and mobile hole-trapped electron, respectively, under 50-kV dc voltage.

Archive of SID
www.SID.ir

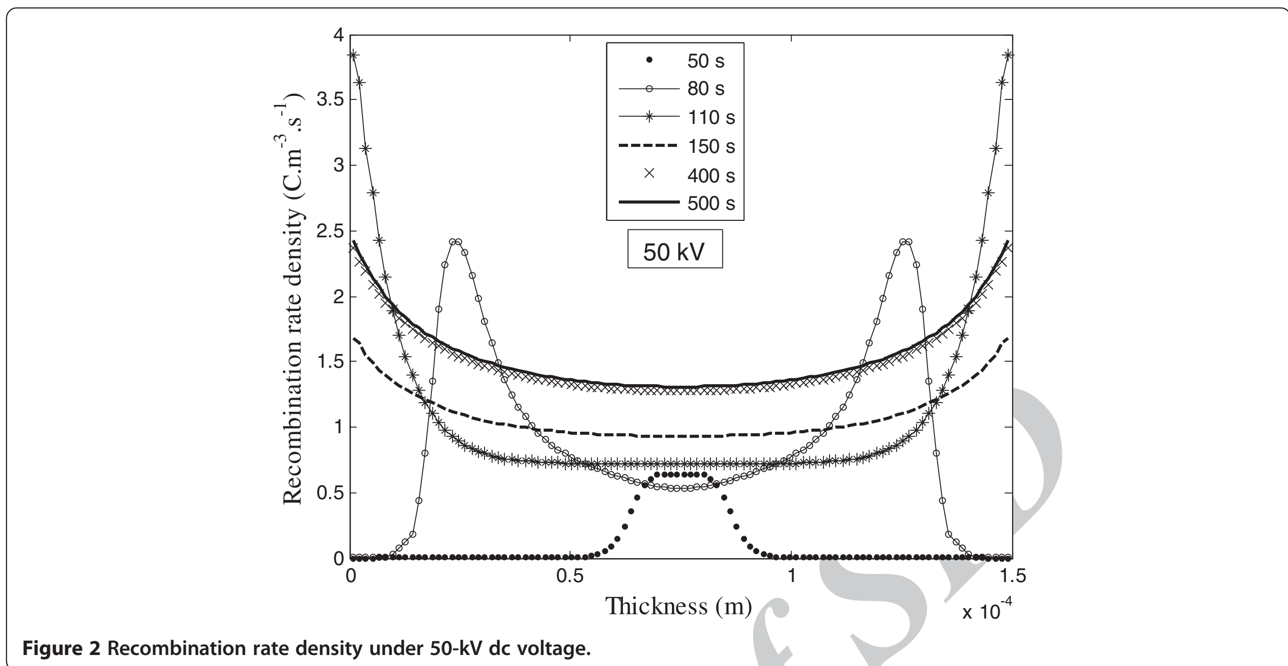

Figure 2 Recombination rate density under 50-kV dc voltage.

This figure indicates that the recombination rates are confined near the anode and the cathode, respectively. This is due to the electron and hole packets which propagate respectively towards the opposite electrode and recombine with trapped holes and trapped electrons which are located close to the anode and the cathode, respectively, as seen in Figure 5a,b.

Figure 6 shows the recombination rate density between the trapped electron-trapped hole under 50-kV dc voltage. This figure indicates rates which are very much lower than those observed in Figure 4a,b. Indeed, if we compare recombination rates near the electrode at 110 s for Figure 4a (or Figure 4b) (3.7 C·m^{-3}·s^{-1}) and Figure 6 (0.027 C·m^{-3}·s^{-1}), we find a ratio that exceeds 100. Finally, we can conclude that, under high dc voltage, total recombination rate density is dominated by the mobile electron-trapped hole and mobile hole-trapped electron recombination. We remember that under high dc voltage, charge dynamic is governed by mobile charges [16,20].

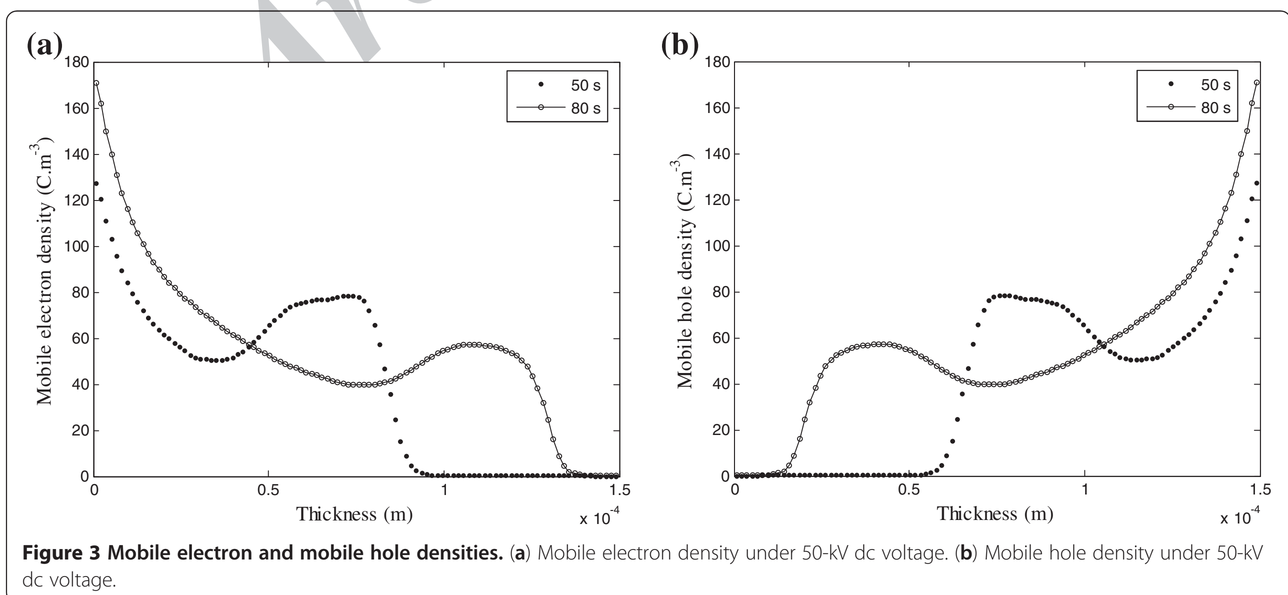

Figure 3 Mobile electron and mobile hole densities. (**a**) Mobile electron density under 50-kV dc voltage. (**b**) Mobile hole density under 50-kV dc voltage.

Archive of SID
www.SID.ir

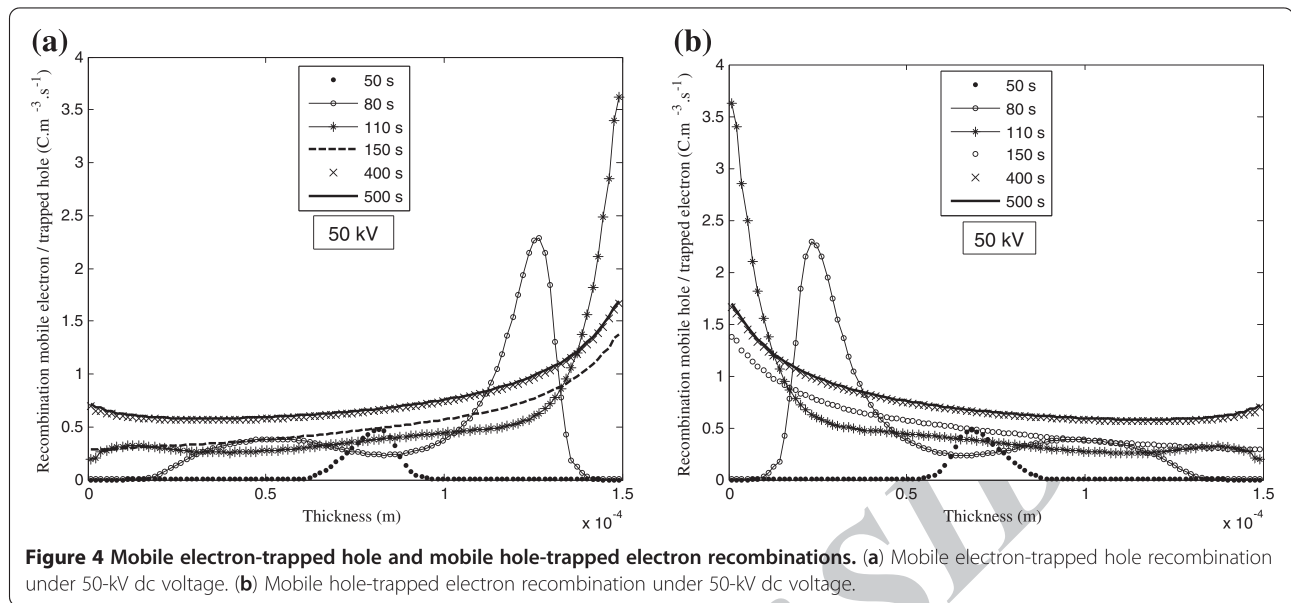

Figure 4 Mobile electron-trapped hole and mobile hole-trapped electron recombinations. (**a**) Mobile electron-trapped hole recombination under 50-kV dc voltage. (**b**) Mobile hole-trapped electron recombination under 50-kV dc voltage.

To explain more this last aspect, we show in Figure 7 the recombination rate density versus time under 50-kV dc applied voltage. Recombination appears after 50 s of applying the voltage and then rapidly increases to a maximum. Then, the recombination rate decreases for a few seconds and increases again until reaching a steady state. This re-increase of recombination rate is due to the re-intensification of the mobile charge injection observed under high voltage [20]. This aspect proves again that total recombination rate density under high dc voltage is dominated by the mobile electron-trapped hole and mobile hole-trapped electron recombination.

Figure 8 shows the total recombination rate density in a LDPE under 1-kV dc applied voltage. At steady state, profiles have concavities that turn to low rates of recombination density (profile 9,000 s), and the recombination rate is highly confined in the middle of the sample. These results are also in a good agreement with those obtained by the steady model of Baudoin [17]. Indeed, under this low voltage, the mobile electron and hole

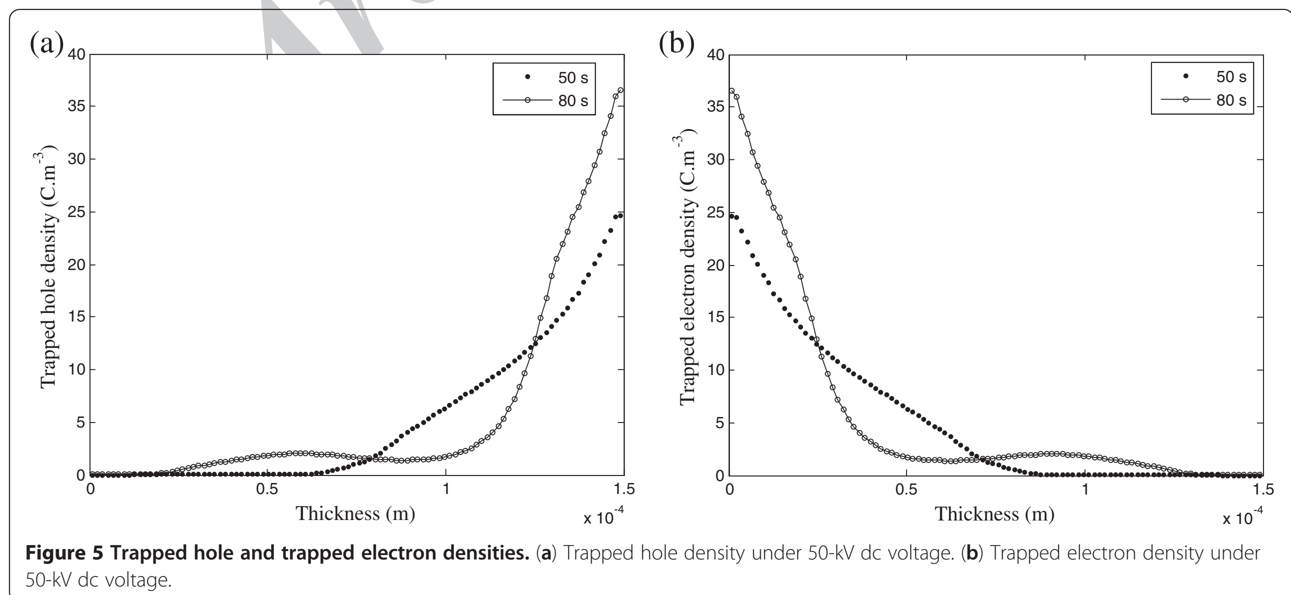

Figure 5 Trapped hole and trapped electron densities. (**a**) Trapped hole density under 50-kV dc voltage. (**b**) Trapped electron density under 50-kV dc voltage.

Archive of SID
www.SID.ir

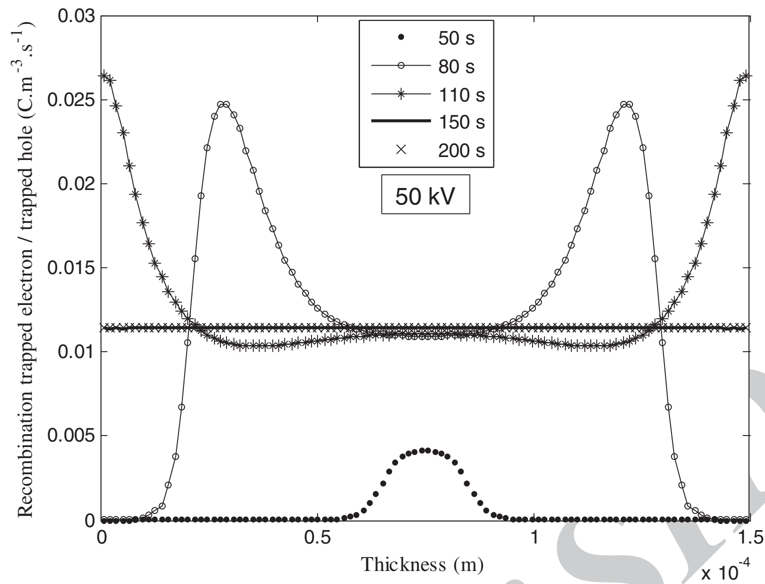

Figure 6 **Trapped electron-trapped hole recombination under 50-kV dc voltage.**

densities are not important and cannot reach the opposite electrodes, so the recombination rate density is more significant in the middle of the sample.

Figure 9a,b shows the recombination rate density, respectively, between the mobile electron-trapped hole and mobile hole-trapped-electron under 1-kV dc voltage. Figure 10 shows the recombination rate density between the trapped electron-trapped hole under 1-kV dc voltage. This last figure indicates rates which are very much higher than those observed on Figure 9a,b. Indeed, if we compare recombination rates at 9,000 s for Figure 10 (1.4×10^{-11} $C{\cdot}m^{-3}{\cdot}s^{-1}$) and Figure 9a (or Figure 9b) (5.4×10^{-13} $C{\cdot}m^{-3}{\cdot}s^{-1}$), we find a ratio that exceeds 25. Finally, we can conclude that, under low dc voltage, total recombination rate density is dominated by the trapped electron-trapped hole recombination. We remember that under low dc voltage, trapped charge density is more important than that of mobile charges as seen in Figure 11a,b [16,20].

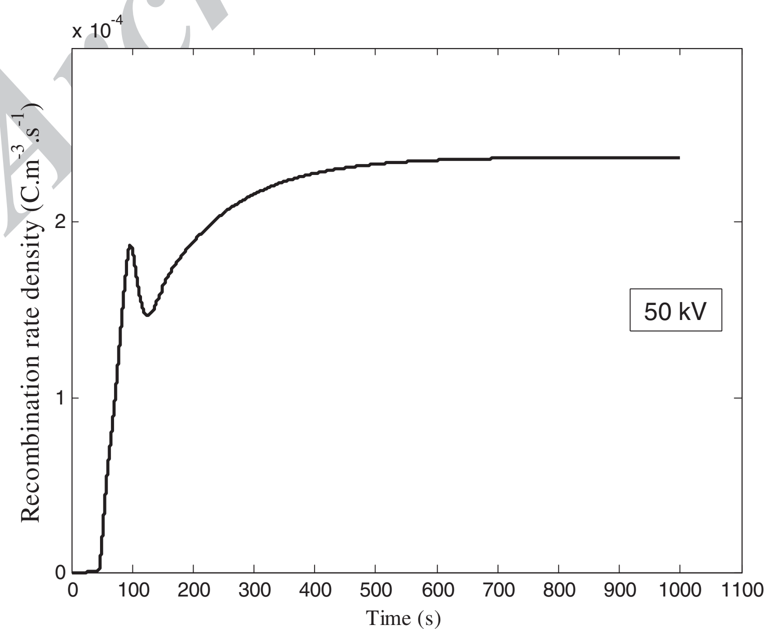

Figure 7 **Recombination rate density versus time under 50-kV dc voltage.**

Archive of SID
www.SID.ir

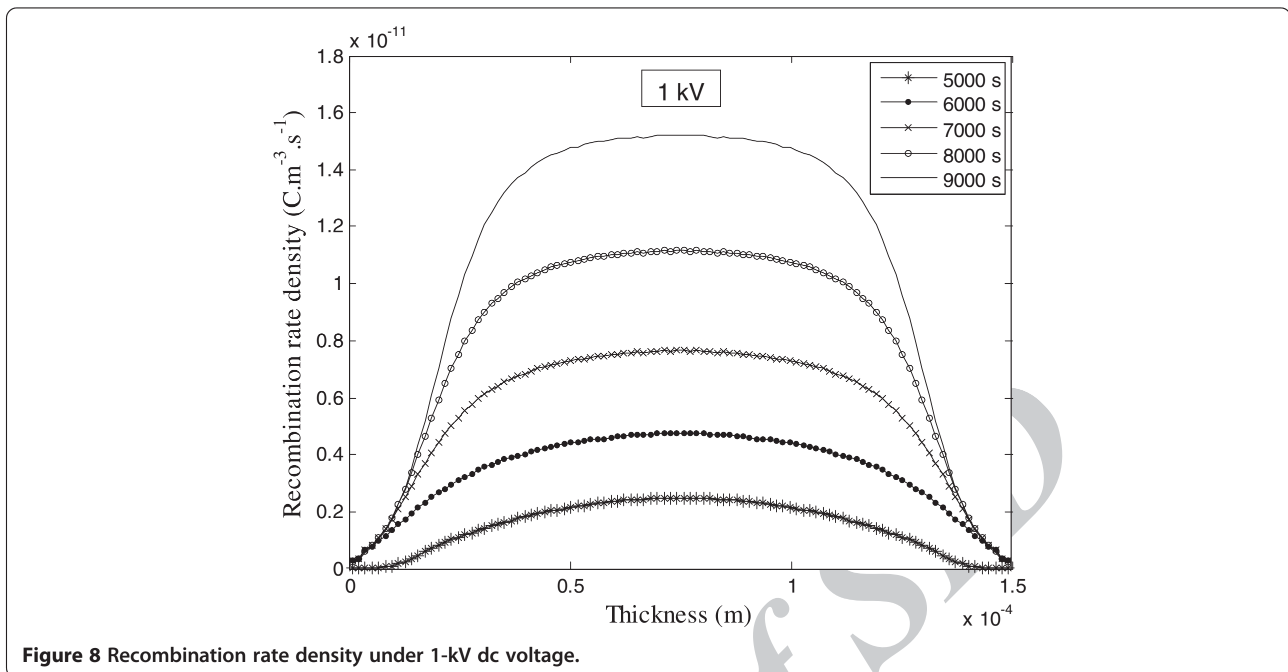

Figure 8 Recombination rate density under 1-kV dc voltage.

Figure 12 shows the recombination rate density versus time under 10-kV dc applied voltage. Recombination appears after 300 s of applying the voltage and rapidly increases to a maximum, and then the recombination rate decreases towards a steady state. This decrease is due to the fact that under low dc voltage, the injection cannot compensate the reduction of mobile charge density under the effect trapping and extraction phenomena [16,20]. This aspect proves again that the total recombination rate density under low dc voltage is dominated by the trapped electron-trapped hole recombination.

Recombination effects on the external current density

Figure 13a,b clearly shows the effect of recombination on the external current evolution. Indeed, the presence of recombination causes the weakening of the current and soon leads to the establishment of the steady state [20]. Indeed, the establishment of recombination induced reduction in

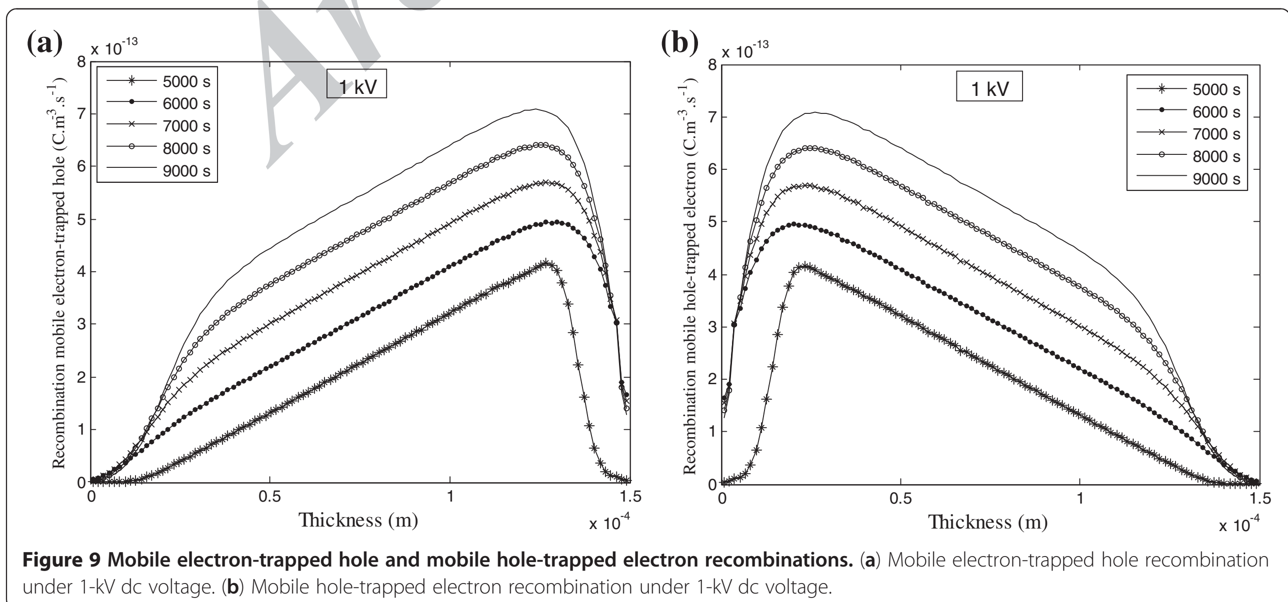

Figure 9 Mobile electron-trapped hole and mobile hole-trapped electron recombinations. (**a**) Mobile electron-trapped hole recombination under 1-kV dc voltage. (**b**) Mobile hole-trapped electron recombination under 1-kV dc voltage.

Archive of SID
www.SID.ir

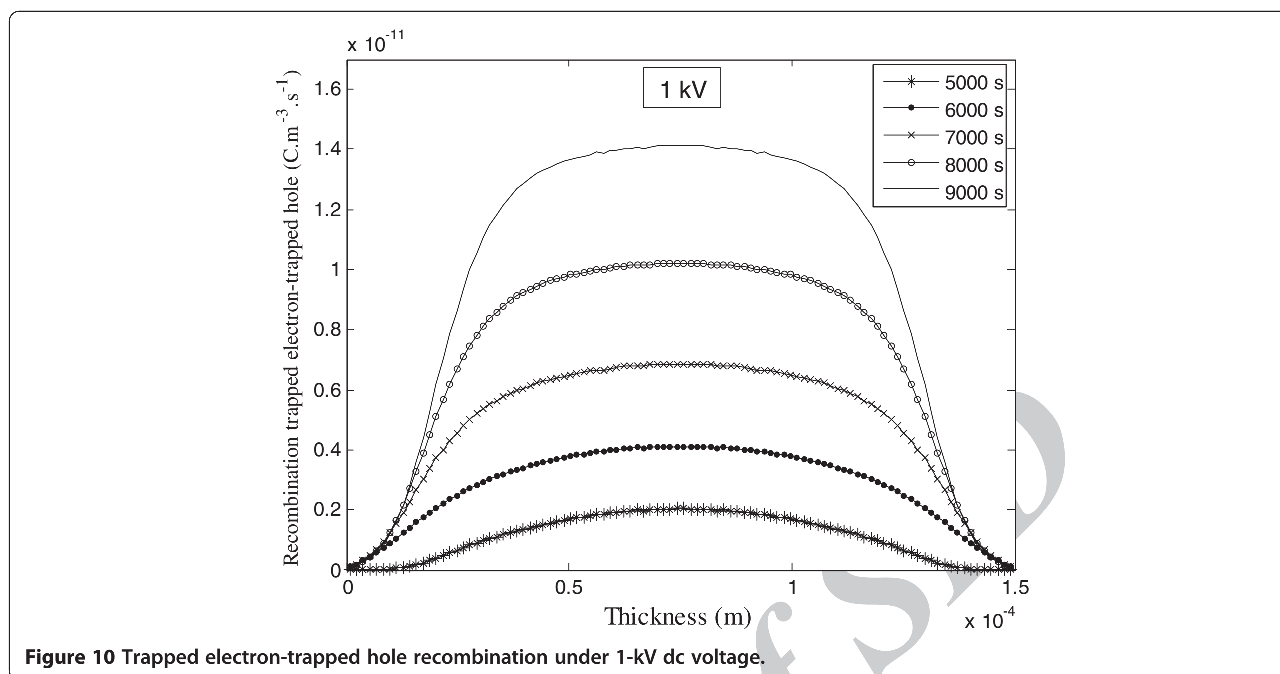

Figure 10 Trapped electron-trapped hole recombination under 1-kV dc voltage.

the density of mobile charges, thus reducing the current density. Whereas without the existence of recombination, the density of mobile charges will be higher, and the current evolution is clearly more important.

We note that the effect of the recombination on the external current density is more significant in the case of high voltage. This is due to the fact that under high voltage, the type of recombination dominating is the recombination between the mobile and trapped charges as shown in the previous section.

We indicate in Figure 13b that the steady state is not established even without recombination because the establishment of steady state requires more time under low voltage [20].

Conclusion

In this paper, we investigated the recombination phenomenon by examining the dominant type of recombination under low and high dc applied voltage. We also examined the effect of recombination on the external

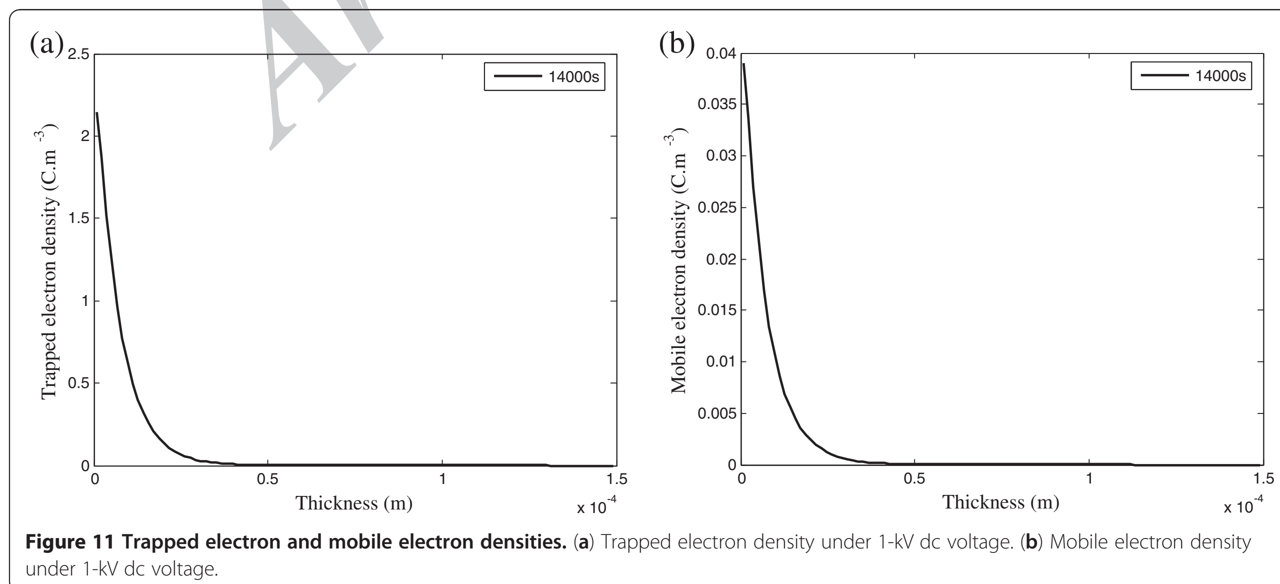

Figure 11 Trapped electron and mobile electron densities. (**a**) Trapped electron density under 1-kV dc voltage. (**b**) Mobile electron density under 1-kV dc voltage.

Archive of SID

www.SID.ir

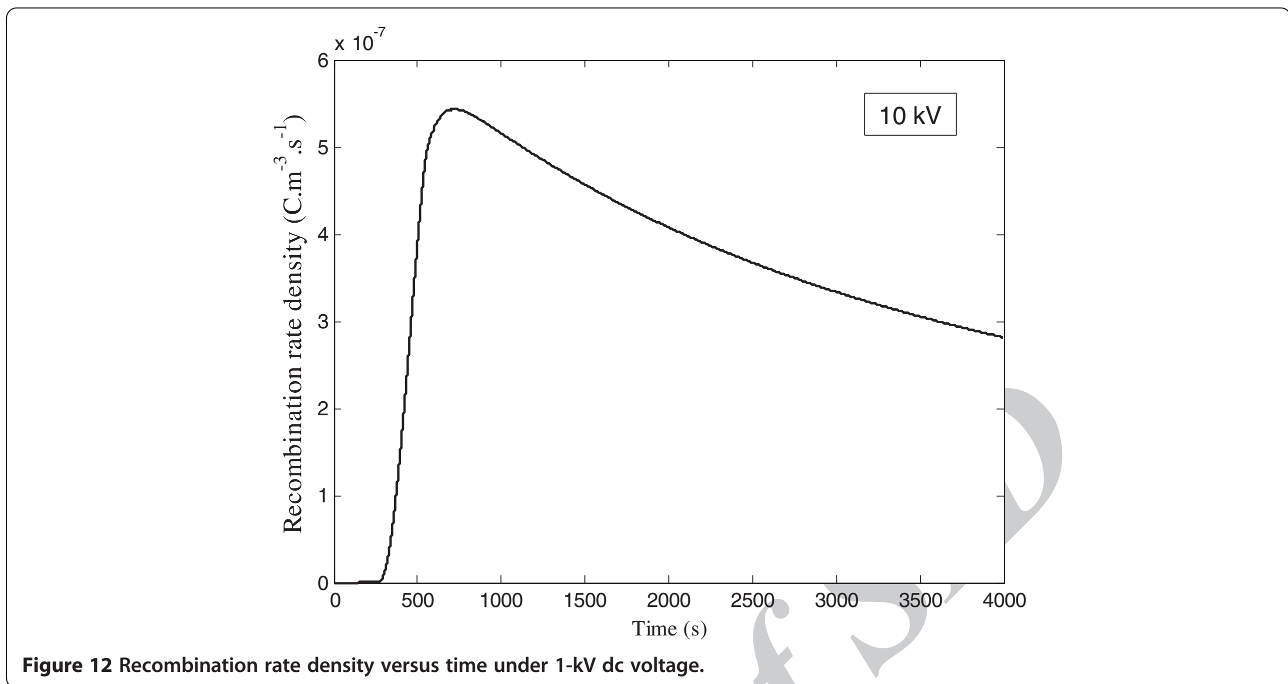

Figure 12 Recombination rate density versus time under 1-kV dc voltage.

current evolution. We showed that under high dc voltage, the recombination rate is highly confined close to the electrodes, and the total recombination rate density is dominated by the mobile electron-trapped hole and mobile hole-trapped electron recombination. Whereas under low dc voltage, the recombination rate is highly confined in the middle of the sample, and the total recombination rate density is dominated by the trapped electron-trapped hole recombination. These results are in a good agreement with those obtained by the steady model of Baudoin. Finally, we proved that the recombination phenomenon causes the decrease of the current and soon leads to the establishment of the steady state, whereas without the existence of recombination, the density of mobile charges will be higher, and the current evolution is more important.

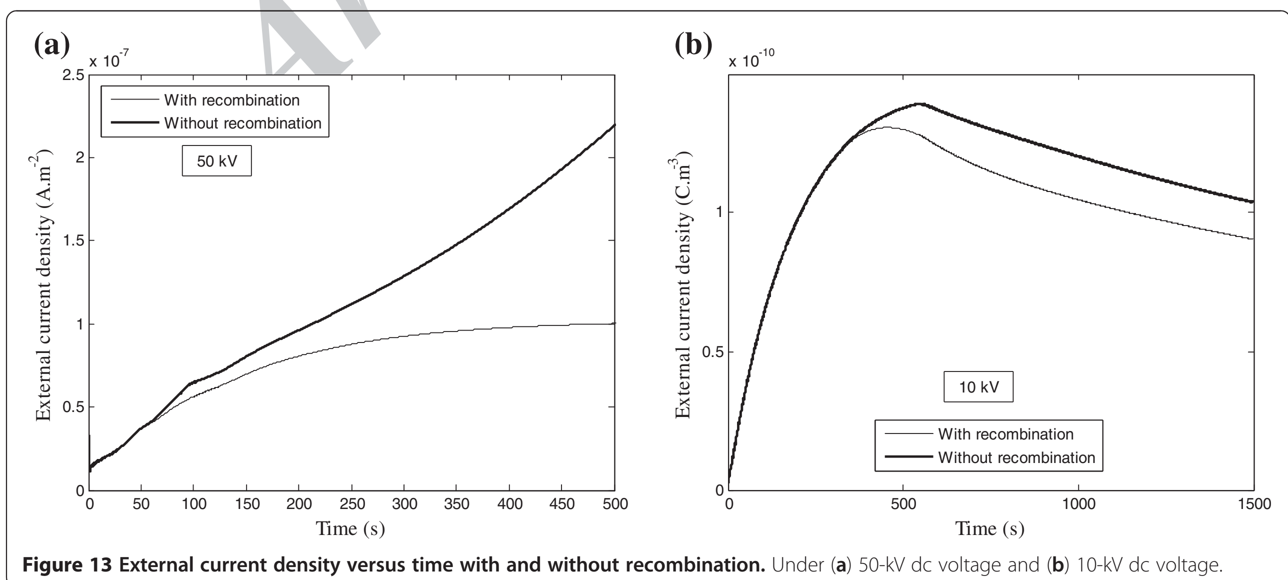

Figure 13 External current density versus time with and without recombination. Under (**a**) 50-kV dc voltage and (**b**) 10-kV dc voltage.

Archive of SID
www.SID.ir

Competing interests
The authors declare that they have no competing interests.

Authors' contributions
IB and EB developed the theoretical part and the modeling program. AG and AK performed the calculation. All authors read the full manuscript and approved it for publication.

Received: 25 October 2012 Accepted: 28 February 2013
Published: 18 April 2013

References
1. Deschamp, L, Caillot, C, Paris, M, Perret, J: Revue Générale de l'Electricité. **5**, 343 (1983)
2. Auclair, H, Dhuicq, B, Favrier, E: Revue Générale de l'Electricité. **3**, 21 (1988)
3. Ridder, E, Monsen, OB: Jicable'99 , 163–168 (1999)
4. Jenni, A, Rengel, U, Meier, A, Osley, J: Jicable'99 , 398–403 (1999)
5. Coelho, R, Aladenize, B: Les diélectriques. Ed. Hermès, Paris (1993)
6. Toureille, A: Mesure de Charges d'espace par la Méthode de l'Onde Thermique: différentes technique de validation numérique et expérimentale. J. Electrostat. **32**, 277–286 (1994)
7. Dissado, LA, Fothergill, JC: Electrical Degradation and Breakdown in Polymers. Peter Peregrinus Ltd, London (1992)
8. Li, Y, Takada, T: Experimental observation of charge transport and injection in XLPE at polarity reversal. J. Phys. D: Appl. Phys. **25**, 704–716 (1992)
9. Tanaka, Y, Li, Y, Takada, T, Ikeda, M: Space charge distribution in low-density polyethylene with charge-injection suppression layers. J. Phys. D: Appl. Phys. **28**, 1232–1238 (1995)
10. Toureille, A: Space charge measurement in solid insulator by the thermal wave method. Revue Générale de l'Electricité **8**, 15–20 (1991)
11. Alison, JM, Hill, R: A model for bipolar charge transport, trapping and recombination in degassed crosslinked polyethene. J. Phys. D: Appl. Phys. **27**, 1291–1299 (1994)
12. Le Roy, S, Segur, P, Teyssedre, G, Laurent, C: Description of charge transport in polyethylene using a fluid model with a constant mobility: model prediction. J. Phys. D: Appl. Phys. **37**, 298–305 (2004)
13. Chen, G, Han Loi, S: Mater. Res. Soc. Symp. **889**, W08-06-1/6 (2006)
14. Kaneko, K, Suzuoki, Y, Mizutani, T: Computer simulation on formation of space charge packets in XLPE films. IEEE Trans. Dielectr. Electr. Insul. **6**, 152–158 (1999)
15. Fukuma, M, Nago, M, Kosaki, M: Computer analysis on transient space charge distribution in polymer. Pro. 4th Int Conf. on Properties and Applications of Dielectric Materials 24–27, Brisbane (1994)
16. Belgaroui, E, Boukhris, I, Kallel, A, Teyssedre, G, Laurent, C: A new numerical model applied to bipolar charge transport, trapping and recombination under low and high dc voltages. J. Phys. D: Appl. Phys. **40**, 6760–6767 (2007)
17. Baudoin, F, Le Roy, S, Teyssedre, G, Laurent, C: Bipolar charge transport model with trapping and recombination: an analysis of the current versus applied electric field characteristic in steady state conditions. J. Phys. D: Appl. Phys. **41**, 025306 (2008)
18. Boukhris, I, Belgaroui, E, Kallel, A: A bipolar transport model for polyethylene films under low dynamics of space charge current. J. Elect. Eng: Theory Appl. **1**, 120 (2010)
19. Boukhris, I, Belgaroui, E, Kallel, A: Post breakdown and lifetime of low density polyethylene film under generated transient charge packets. Eur. Phys. J. Appl. Phys. **60**, 10203 (2012)
20. Belgaroui, E, Boukhris, I, Kallel, A: Transient and steady-state currents in polyethylene film under low and high dc voltages. Eur. Phys. J. Appl. Phys. **48**, 20404 (2009)

doi:10.1186/2251-7235-7-18
Cite this article as: Boukhris et al.: **Recombination phenomenon in polyethylene under space charge dynamics and its effects on the external current evolution.** *Journal of Theoretical and Applied Physics* 2013 7:18.

Submit your manuscript to a SpringerOpen journal and benefit from:

► Convenient online submission
► Rigorous peer review
► Immediate publication on acceptance
► Open access: articles freely available online
► High visibility within the field
► Retaining the copyright to your article

Submit your next manuscript at ► springeropen.com

Archive of SID
www.SID.ir